Comparisons of Algorithm Products Between Experimental and Current WSR-88D Volume Coverage Patterns Used in the 2002 KBIX Field Test

Rodger A. Brown[1], Bradley A. Flickinger[1,2], and Vincent T. Wood[1]

[1]National Severe Storms Laboratory
[2]Cooperative Institute for Mesoscale Meteorological Studies
Norman, Oklahoma

Final Report

Task 2.2

FY 2003 Memorandum of Understanding Between
Radar Operations Center
and
National Severe Storms Laboratory

22 January 2003

Executive Summary

Following installation of radars in the WSR-88D network, National Weather Service forecasters began requesting scanning strategies that are faster and that have greater vertical resolution at lower elevation angles. Faster scanning is needed to better monitor fast-evolving severe weather events such as tornadoes and microbursts. Greater vertical resolution at lower elevation angles is needed to provide more accurate surface precipitation estimates, provide better confirmation of microburst and circulation signatures, and provide sufficient data at middle and far ranges to activate severe storm algorithms. During the past several years, the Radar Operations Center and National Severe Storms Laboratory (NSSL) have been investigating experimental volume coverage patterns (VCPs) that will provide forecasters with more informative severe weather data.

This report discusses findings from a field test of experimental VCPs conducted during April-June 2002 using Keesler Air Force Base's WSR-88D (KBIX) near Biloxi, Mississippi. In order to verify improved algorithm performance (using NSSL versions of WSR-88D algorithms) with the experimental VCPs, comparisons were made between (a) KBIX using the experimental VCPs and (b) one of three nearby WSR-88Ds using current VCPs 11 and 21. Comparisons were made only for those storms that were approximately equidistant from both radars. Owing to the locations of the radars, only storms at middle to far ranges (that is, greater than about 100 km or 55 n mi) from KBIX were equidistant long enough to do meaningful comparisons.

Basic findings show that the greater vertical resolution of experimental VCPs makes a difference between identification and nonidentification of a severe storm by the various severe storm algorithms. When cells or circulations leading to mesocyclones are identified using both current and experimental VCPs, this study indicates that the features are identified up to 10-35 min earlier with experimental VCPs. Once a cell is identified, the appropriate algorithms start producing information and trends concerning parameters such as cell track, maximum reflectivity, vertically integrated liquid (VIL), probability of hail and severe hail, and maximum hail size. Once a circulation is identified, the forecaster is alerted to the fact that a mesocyclone may form with its associated strong winds, large hail, and possibility for tornadoes.

It is argued that experimental VCP Gamma would have the most overall impact on the operational community and, therefore, should be implemented first. This VCP is a faster version of VCP 11, where elevation angles are optimized to provide better surface precipitation estimates and better low-altitude vertical resolution resulting in earlier identification of damage-producing storms.

1. Introduction

In response to requests by forecasters for WSR-88D volume coverage patterns (VCPs) that are faster and have finer vertical resolution at low elevation angles, the Radar Operations Center (ROC) and National Severe Storms Laboratory (NSSL) have developed a set of experimental VCPs that satisfy the forecasters' needs. The VCPs have been made faster by increasing the antenna rotation rate, especially at higher elevation angles; however, the rotation rates are slow enough to maintain data quality consistent with system specifications. Maximum rotation rates are less than 5 revolutions per minute, which permit the standard errors of estimate of reflectivity and Doppler velocity to not exceed specified threshold values of 1 dBZ and 1 m s^{-1}, respectively. Finer vertical resolution has been achieved by shifting the elevation angles, except the lowest one, slightly downward.

The experimental VCPs have been given interim names based on the Greek alphabet: Alpha, Beta, Gamma, Delta, Epsilon, and Zeta. Characteristics of these VCPs are listed below.

VCP Alpha - Clear Air Mode completing 9 unique elevation angles from 0.5 to 4.9° in 10 min (making separate reflectivity and Doppler velocity scans at the lowest three elevation angles).

VCP Beta - Shallow/Distant Convection Mode completing 12 unique elevation angles from 0.5 to 8.1° in 5 min (making separate reflectivity and Doppler velocity scans at the lowest three elevation angles).

VCP Gamma - Deep Convection Mode (modified VCP 11) completing 14 unique elevation angles from 0.5 to 19.5° in 4.1 min (making separate reflectivity and Doppler velocity scans at the lowest two elevation angles).

VCP Delta - Fast Evolution Mode (designed for tornado and microburst monitoring) completing 6 unique elevation angles from 0.5 to 6.5° in 2.3 min (making separate reflectivity and Doppler velocity scans at the lowest three elevation angles).

VCP Epsilon - Multiple Pulse Repetition Frequency (PRF) Deep Convection Mode completing 12 unique elevation angles from 0.5 to 19.5° in 5 min (making one reflectivity and three Doppler velocity scans, each with a different PRF, at each of the lowest three elevation angles).

VCP Zeta - Multiple PRF Fast Evolution Mode completing 5 unique elevation angles from 0.5 to 6.5° in 3.3 min (making one reflectivity and three Doppler velocity scans, each with a different PRF, at each of the lowest three elevation angles).

The multiple PRF scans at lower elevation angles for VCPs Epsilon and Zeta are short-term software solutions for eventual hardware solutions (ORDA Enhancement Project) that will further reduce range folded data and improperly dealiased Doppler velocity data. A study of multiple PRF data is ongoing and is not discussed here.

During the spring of 2002, a field test of the experimental VCPs was conducted in the

southern half of Mississippi and portions of adjacent Louisiana and Alabama. Most of the experimental VCP data collected during the field test were with VCPs Beta and Gamma. Primary differences between current VCPs 11 and 21 and the experimental VCPs are in the vertical spacings between elevation angles at lower angles. Differences between the lower elevation angles of VCPs 11 and 21 (Fig. 1) are one (half-power) beamwidth (0.9-1.0°), while those of VCPs Beta and Gamma (Fig. 2) are one-half (half-power) beamwidth (0.4-0.5°). The four lowest elevation angles of VCPs 11 and 21 are the same and the five lowest angles of VCPs Beta and Gamma are essentially the same. As will be shown, the more closely spaced lower elevation angles of the experimental VCPs have a pronounced effect on the identification of storms at middle and far ranges from a radar.

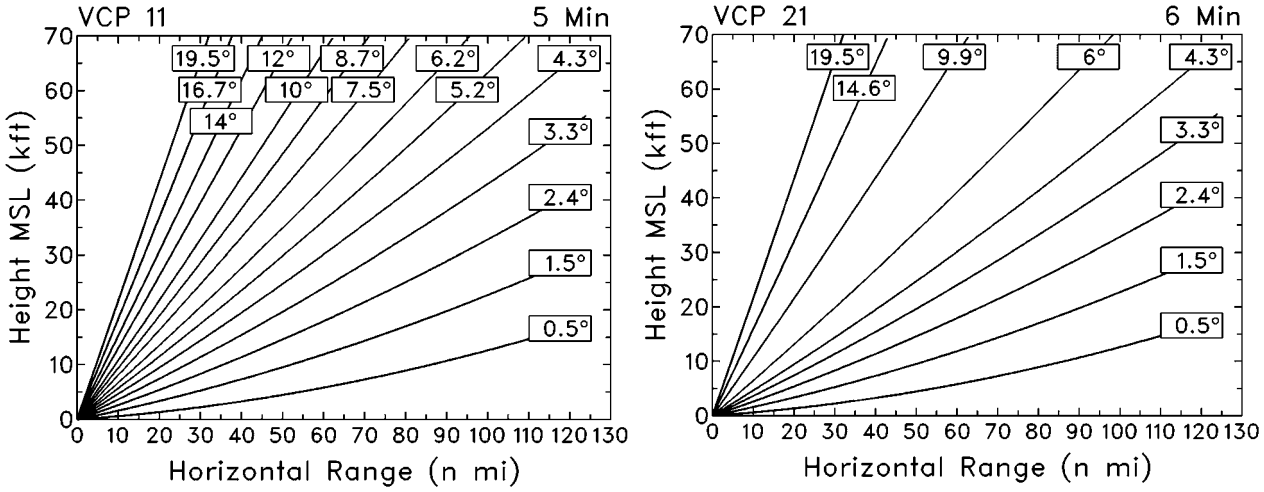

Figure 1. Current VCPs 11 and 21.

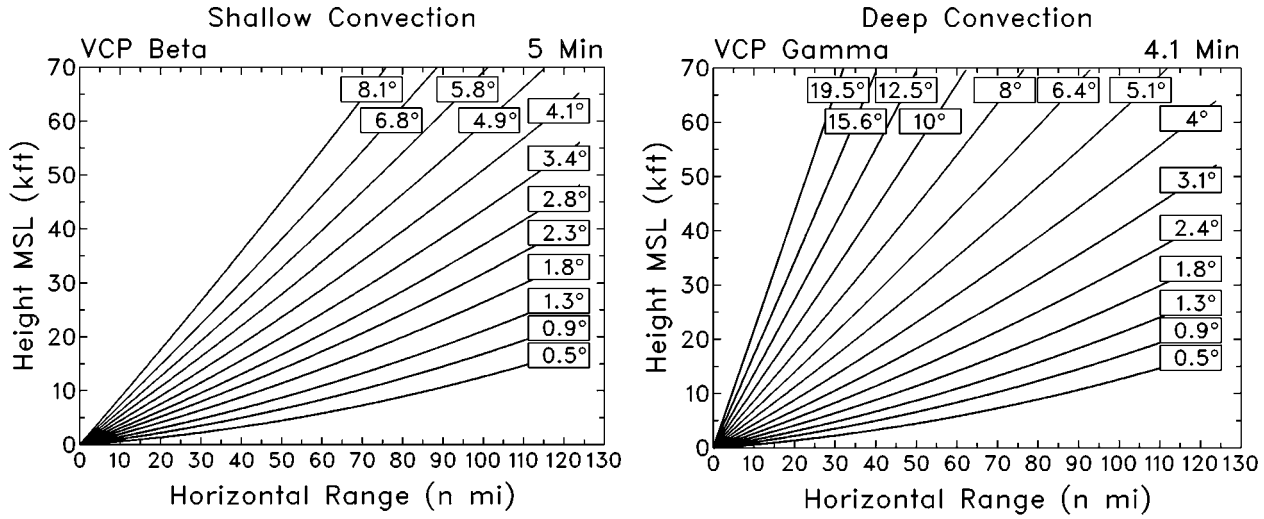

Figure 2. Experimental VCPs Beta and Gamma.

2. Field Test of the Experimental VCPs

The field test of experimental VCPs was conducted during April-June 2002 using WSR-88D KBIX at Keesler Air Force Base near Biloxi, MS. The radar was operated remotely from a control center at NSSL in Norman, OK and compressed radar data were transmitted back to the control center for viewing, recording, and subsequent data analysis.

For analysis purposes, radar data collected by KBIX using experimental VCPs were compared with current VCPs 11 and 21 collected by the Slidell, LA (KLIX), Jackson, MS (KJAN), and Mobile, AL (KMOB) WSR-88Ds (see Fig. 3). The Jackson National Weather Service (NWS) Forecast Office recorded data from all three operational WSR-88Ds and shipped tapes at periodic intervals to the ROC.

During the three-month field test, nearly 9,000 volume scans were recorded for KBIX. Although data were collected using all six experimental VCPs, most data were collected using VCPs Beta (55%) and Gamma (32%).

Figure 3. Map of the field test area.

The following nine days were chosen for comparing algorithm output between KBIX and one of the nearby WSR-88Ds :

8 April 2002	Tornado, Hail, Wind
29 April 2002	Hail, Wind
30 April 2002	Hail, Wind
3 May 2002	Wind
9 May 2002	Hail
17 May 2002	Hail, Wind
30 May 2002	Wind
4 June 2002	Wind
20 June 2002	Hail, Wind

These days were chosen based on the existence of severe weather reports within the KBIX coverage area and the availability of data tapes from KBIX and at least one other WSR-88D.

3. Comparison Procedures

Analyses of data collected during the field test consisted of comparisons of NSSL versions of WSR-88D algorithm products between the current and experimental VCPs. The following Warning Decision Support System II (WDSS II) algorithms were used: Storm Cell Identification and Tracking (SCIT) Algorithm, Hail Detection Algorithm, Mesocyclone Detection Algorithm, and Tornado Detection Algorithm. Grid-based vertically integrated liquid (VIL) was obtained from the Open Radar Product Generator (ORPG) version of the VIL Algorithm and cell-based VIL was obtained from the WDSS II SCIT Algorithm.

The comparisons were made for storms located at approximately the same distances from KBIX and one of the three nearby WSR-88Ds; that is, both of the radars had similar-sized antenna beamwidths that measured similar resolution scales. Owing to the relative locations of the radars, comparisons were made only for those storms beyond about 100 km (55 n mi).

Figure 4 shows geographical distributions of differences in distance from KBIX and from each of the three nearby WSR-88Ds. For example, in Fig. 4a, the band with darkest shading midway between KBIX and KJAN is the region where distances from the two radars differ by 10% or less. Similar regions between KBIX and KLIX and between KBIX and KMOB are shown in Figs. 4b and 4c, respectively. Comparisons of algorithm outputs between radars were limited to regions where the distances from a pair of radars were within 10% of each other. In addition, since KLIX and KMOB are within 100 km of KBIX, no algorithm comparisons were made within the radars' "cones of silence", that is, within 50 km of each radar.

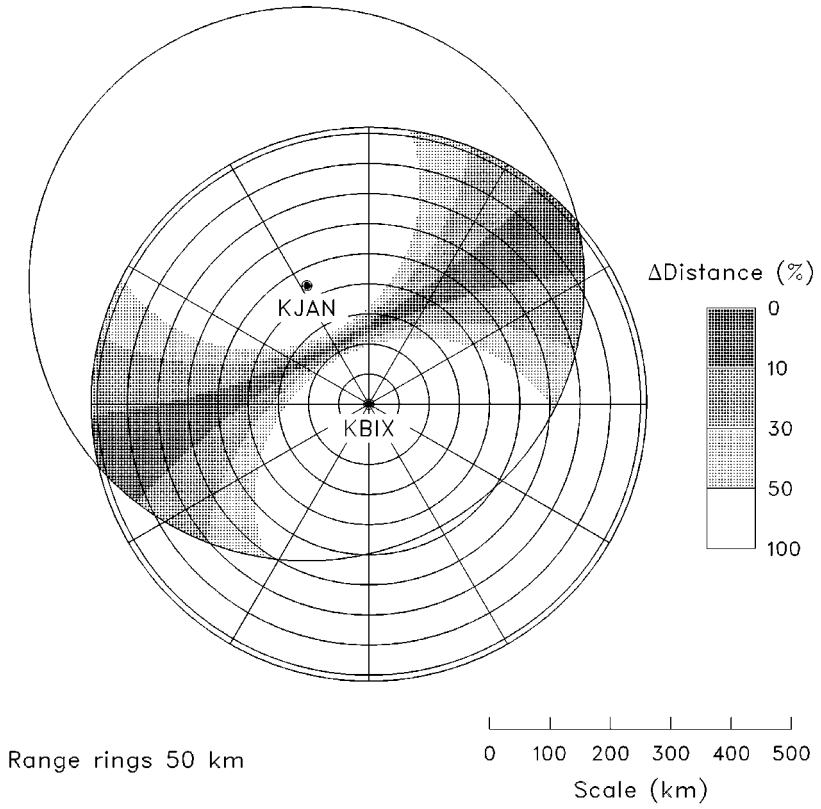

Figure 4a. Geographic distribution of percentage differences in distance from KBIX and KJAN within 460 km (250 n mi) of both radars. Darkest shading indicates locations where distances from the two radars are within 10% of each other.

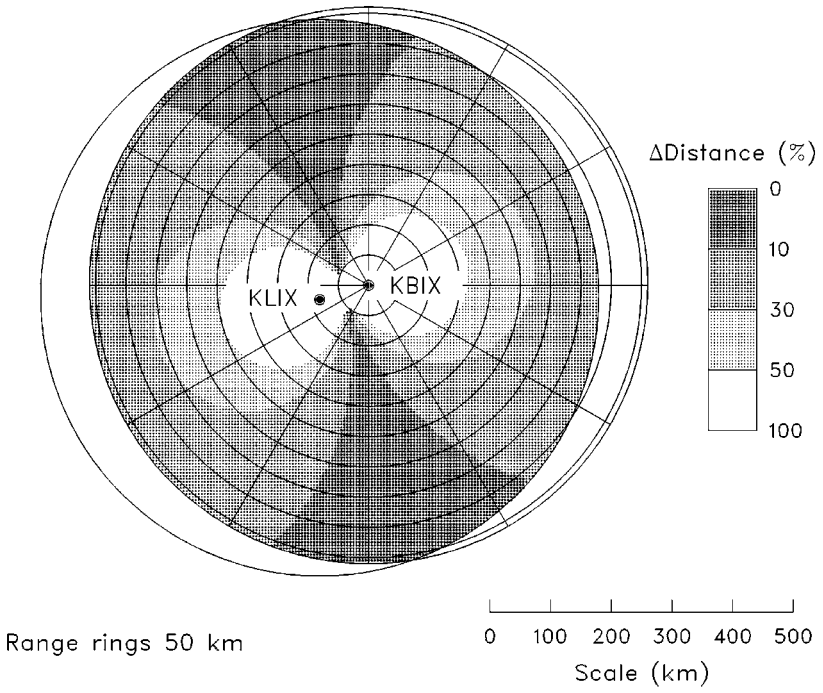

Figure 4b. Same as Fig. 4a, except for KBIX and KLIX. The blank region within 50 km of each radar represents the "cone of silence" where no comparisons were made.

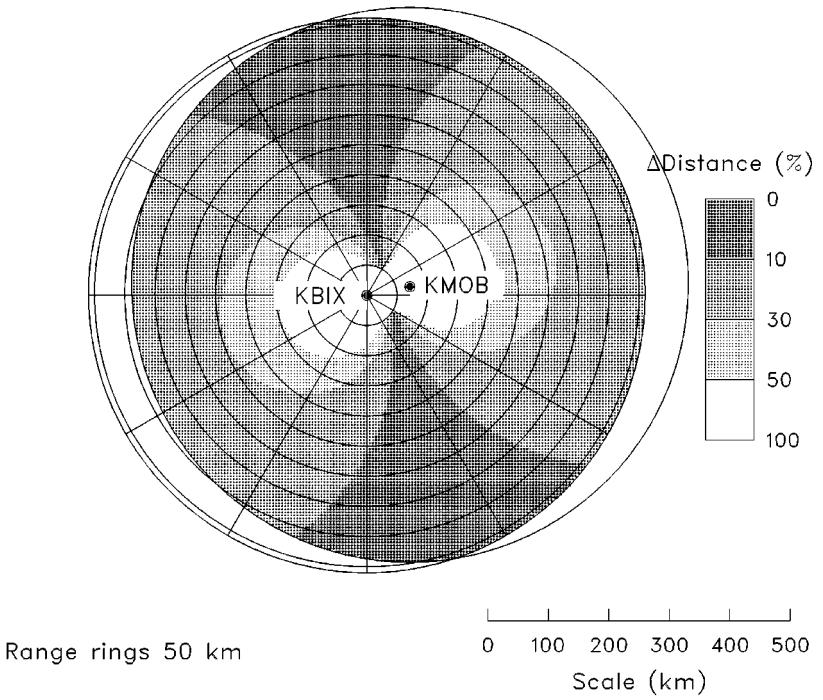

Figure c. Same as Fig. 4b, except for KBIX and KMOB.

4. Comparative Results From Field Test

a. Mesocyclones and tornadoes

Very few mesocyclones or tornadoes occurred within 230 km (125 n mi) of KBIX during the three-month test period. The only day with recorded measurements during the reported occurrence of tornadoes was 8 April 2002, when a squall line passed through the area. Though there were some tornadic vortex signatures (TVSs), it was difficult to correlate reports of the short-lived tornadoes with short-lived TVSs from any of the radars. This is a common problem with vortices that form along the leading edge of a squall line. In addition, reported tornado times may be in error and measurements from the Slidell radar, which was closest to the reported tornadoes, indicate that there were some data quality problems. Therefore, it was not possible to make any tornado comparisons.

On 29 April 2002, there were several mesocyclones identified by the Mesocyclone Detection Algorithm within 230 km of KBIX. Two of these mesocyclones were roughly equidistant from KBIX and one or more of the nearby WSR-88Ds. Figure 5 shows tracks

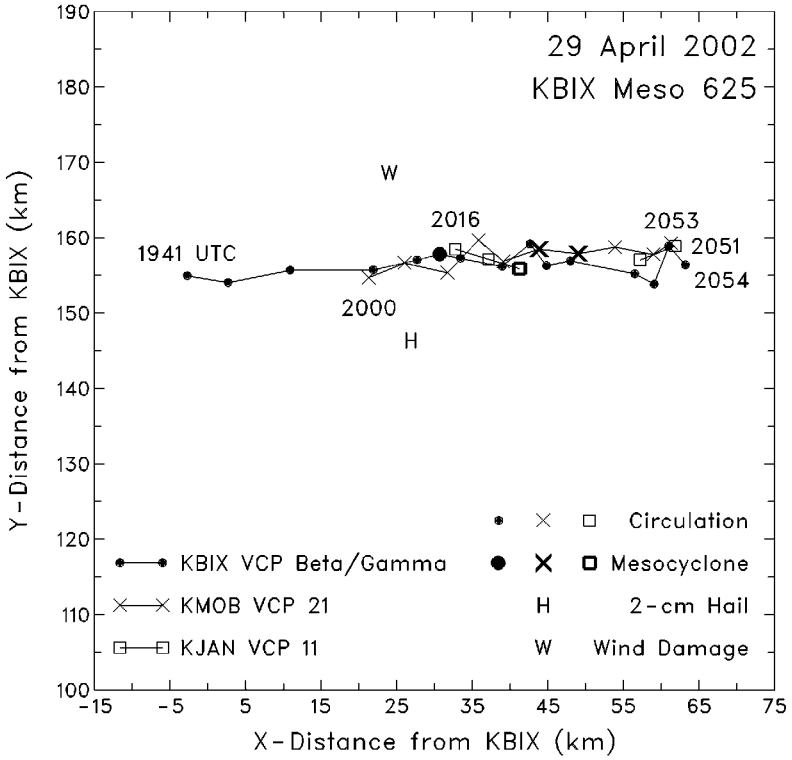

Figure 5. Tracks of the circulation that produced Mesocyclone 625 (KBIX) as seen by three radars. Larger symbols along the track indicate the identification of mesocyclone signatures. The KJAN track has a break in it. Locations of damaging wind and hail reports from Storm Data *are noted.*

of a circulation identified by KBIX, KMOB, and KJAN that briefly produced a mesocyclone

signature. (At the times of the mesocyclone signatures, range differences were about 10% or less; however, the differences were greater than 10% along other portions of the tracks.). The algorithm identified a circulation in the KBIX Doppler velocity field (VCPs Beta and Gamma) about 20 min before one was identified in the KMOB data (VCP 21) and 35 min before one was identified in the KJAN data (VCP 11). The mesocyclone signatures occurred at slightly different times for the three radars, with the circulation reaching mesocyclone strength (Rank 5) 12-16 min earlier in the KBIX data. The circulation tracks based on the three radars are very similar. After the 2054 volume scan, KBIX switched to an MPDA VCP, so continuity on the circulation was lost and no data from the other radars were plotted.

A second mesocyclone occurred a couple of hours later (Fig. 6). The algorithm identified a circulation in the KBIX Doppler velocity field (VCP Beta) 16 min before one was identified in the KLIX data (VCP 21) and the identification lasted 10 min longer with VCP Beta. The detected strength of the circulation reached Rank 5 about 10 min earlier with VCP Beta. It is impressive in these two examples that the experimental VCPs, with their more closely spaced lower elevation angles, can identify circulations 15-35 min earlier and identify the presence of mesocyclones 10-15 min earlier than the current VCPs.

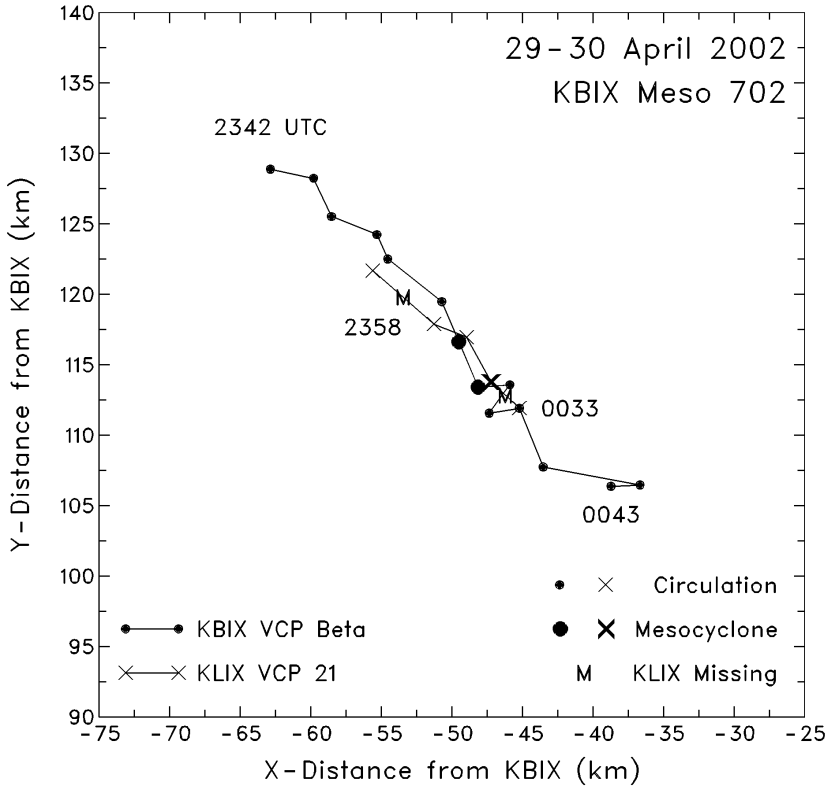

Figure 6. Track of the circulation that produced Mesocyclone 702 (KBIX) as seen by KBIX and KLIX. Bolder symbols along the track indicate identification of a mesocyclone signature.

b. Maximum reflectivity

The temporal evolution of maximum reflectivity within a cell was obtained from the Storm Cell Identification and Tracking (SCIT) Algorithm. Plotted in Fig. 7 are curves showing reflectivity evolution in KBIX Cell 33 on 4 May 2002 based on measurements from KBIX (VCP Beta) and KMOB (VCP 21). Average distance from the two radars varied from 140 to 150 km (75-80 n mi). The SCIT algorithm identified the cell 12 min earlier with VCP Beta. Overall lifetime of the identified cell was 17 min longer with VCP Beta than with VCP 21.

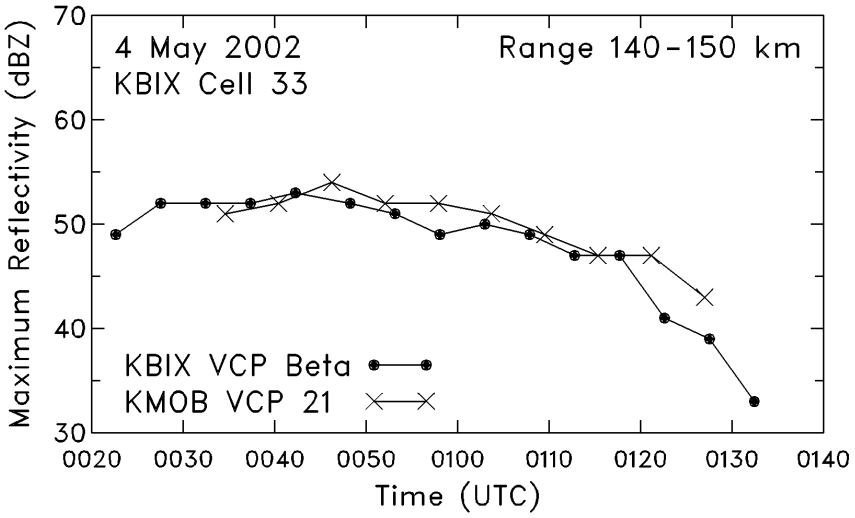

Figure 7. Temporal variation of maximum reflectivity within a cell identified by KBIX using VCP Beta and KMOB using VCP 21.

Plotted in Fig. 8 are curves showing temporal variation of maximum reflectivity associated with the early portion of KBIX Cell 5 on 29 April 2002 at greater average ranges of 170-190 km (90-100 n mi). The SCIT Algorithm identified the storm over 35 min earlier with KBIX using VCP Beta than with KMOB using VCP 21. By the time KMOB began to identify the storm, the hail algorithm using VCP Beta had been indicating for 25 min that the storm had up to 70% probability of producing hail (not shown). Note that the finer vertical resolution of VCP Beta at this range produces less temporal variation in maximum reflectivity values compared with VCP 21 after 1910.

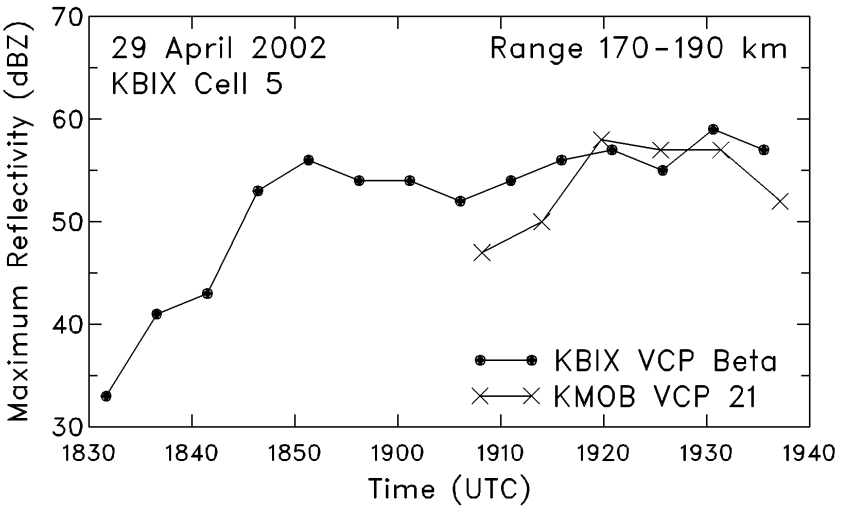

Figure 8. Temporal variation of maximum reflectivity within a cell identified by KBIX using VCP Beta and by KMOB using VCP 21.

Maximum reflectivities were tabulated for 46 cells that occurred equidistant (i.e., within ±10%) from KBIX (using experimental VCPs) and one of the nearby radars (using current VCPs) and that were identified by the SCIT Algorithm for at least 15 min using KBIX data. There were times when the early and late portions of cells were identified only by KBIX. For those times when cells were identified by two radars, the differences in maximum reflectivities between KBIX and the nearby radar were computed. Since the time to complete a volume scan differed between KBIX and the nearby radars, the reflectivity value at the time closest to the KBIX time was used to compute the reflectivity difference.

Reflectivity differences are plotted in Fig. 9 as a function of the average range for each radar pairing. There were roughly the same number of KBIX-KLIX and KBIX-KMOB pairings, but much fewer KBIX-KJAN pairings because the equidistant coverage area was much more limited (see Fig. 4). As seen in Fig. 9, comparisons were made for cells ranging from 100 km to more than 350 km (55-190 n mi) from the radars. The distributions of data points suggest that KBIX reflectivities were greater than KJAN values, but that KBIX values were less than KLIX and KMOB values. These speculations are confirmed in Table 1, which shows the mean and standard deviation for each radar pairing. The standard deviations of the reflectivity differences for all three pairs are essentially the same (3.6-4.4 dBZ). However, the means of the difference values suggest that there may be calibration differences among the four radars–even though all four radars were calibrated by ROC personnel prior to the field test. For example, maximum reflectivities from KJAN are about 5.0-5.5 dBZ less than those from KLIX and KMOB.

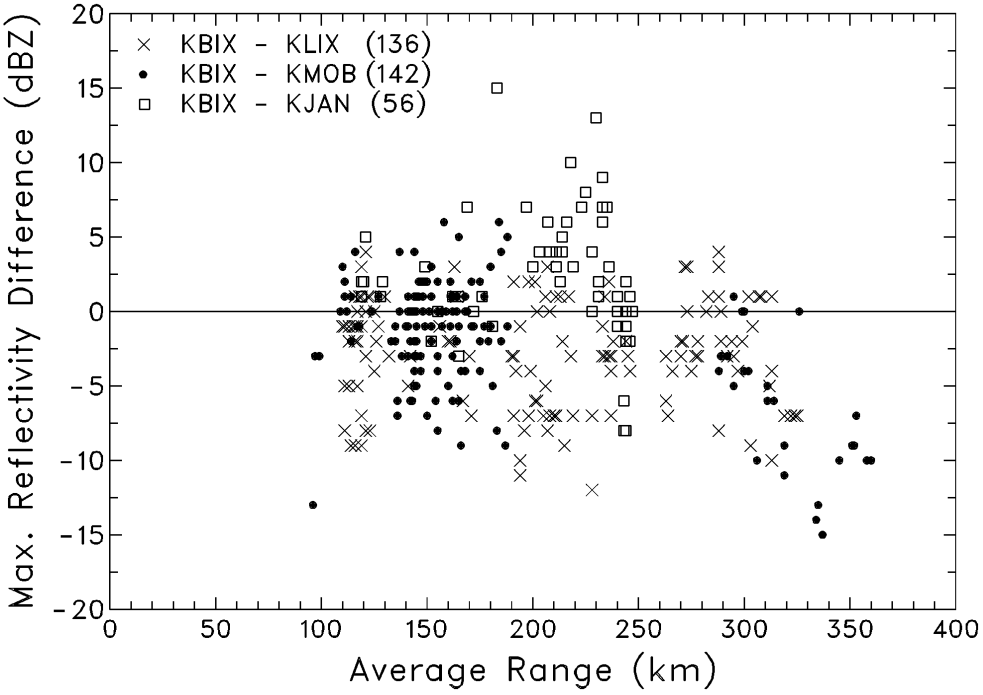

Figure 9. Scatter plot, as a function of average range of each radar pair, of the differences in maximum reflectivity in a given cell between KBIX and each of the three nearby radars. The number of difference values for each radar pair is indicated in parentheses.

Table 1. Means and standard deviations of maximum reflectivity differences between KBIX and nearby WSR-88Ds.

Radar Pair	Mean Difference	Standard Deviation
KBIX-KLIX	-2.85 dBZ	3.59 dBZ
KBIX-KMOB	-2.11 dBZ	4.09 dBZ
KBIX-KJAN	2.59 dBZ	4.36 dBZ

KJAN has a beam blockage problem in the azimuth sector from about 045° through 120°,

so blockage could contribute to lower reflectivity values. To investigate this possibility, the KBIX-KJAN differences in maximum reflectivity were divided into two groups: one where the azimuths of the maximum values were within the 045º to 120º blocked sector (45% of the data) and the other where the azimuths were in the unblocked sector (55% of the data). The results of this comparison are shown in Table 2. It is seen that the mean maximum reflectivity measured by KJAN in the blocked sector is 3.9 dBZ lower than the mean value for KBIX, while the mean value is only 1.5 dBZ lower in the unblocked sector. Using the unblocked value, the mean KJAN measurement is still about 4 dBZ lower than the KLIX and KMOB values. The distributions of maximum reflectivity differences, as reflected by the standard deviation values, among the various radars are much more uniform using the unblocked difference for KJAN. Standard deviation values range from 3.59 to 4.09 dBZ, compared to a range from 3.59 to 4.36 dBZ when data from the blocked azimuths are included.

Table 2. Mean and standard deviation of the KBIX-KJAN maximum reflectivity difference for KJAN azimuthal sectors with and without beam blockage.

Sector	Mean Difference	Standard Deviation
Blocked	3.92 dBZ	4.46 dBZ
Unblocked	1.52 dBZ	4.04 dBZ

It might be informative to investigate those situations where cells were identified with KBIX data but were not identified with data from the equidistant radar. In particular, one might wonder about the strength of those cells that were not identified by the SCIT Algorithm for the nearby radars. Plotted in Fig. 10 are the maximum reflectivities in KBIX cells that were not identified at the same time by an equidistant nearby radar. Although a relatively small sample (about 230 volume scans) was available, data in Fig. 10 indicate that there were cells with maximum reflectivities greater than 50 dBZ at all ranges that the SCIT Algorithm did not identify in the nearby radar data. The reason for missed identification apparently was that the cells were detected only at the lowest elevation angle of the current VCP. With the more closely spaced lower elevation angles of the experimental VCPs, KBIX cells were detected at two or three elevation angles, enough to be identified by the SCIT Algorithm.

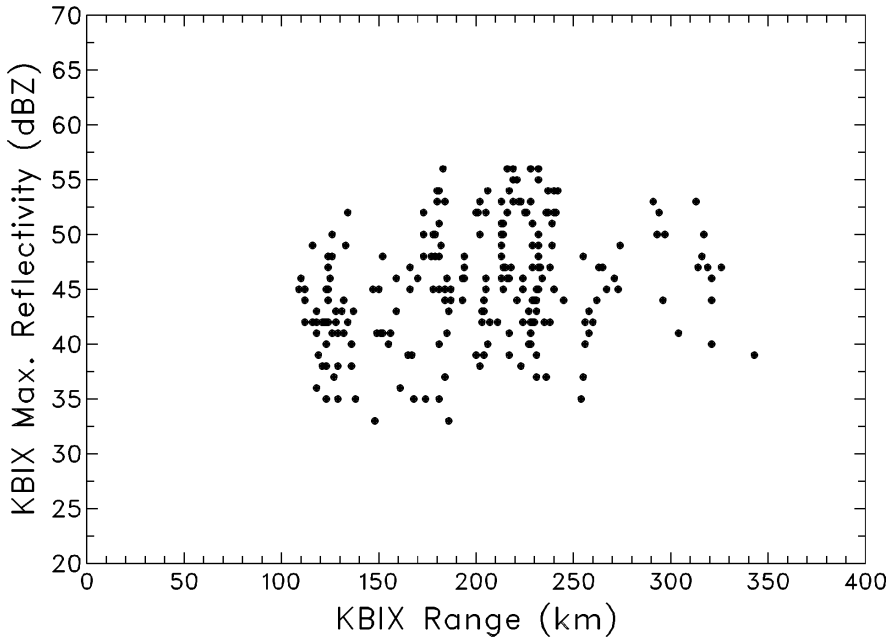

Figure 10. Maximum reflectivities from the SCIT Algorithm measured by KBIX (using experimental VCPs) for cells that were not identified by KLIX, KJAN, or KMOB (using the current VCPs).

c. Echo tops

In addition to making comparisons with the nearby radars, occasionally the observers in the control room changed KBIX from an experimental VCP to VCP 11 or 21. In this way, direct comparisons could be made using adjacent volume scans. An example of echo top comparisons is shown in Fig. 11 For the strongest storm located about 220 km (120 n mi) north of KBIX, echo top based on VCP 21 is 15 kft (4.5 km) MSL, while echo top based on VCP Beta is 25 kft (7.5 km). The VCP 21 echo top is lower because the storm was detected only at the lowest elevation angle (0.5°); only one elevation angle is required for computation of echo top heights. On the other hand, VCP Beta detected the storm using the lowest three elevation angles (0.5°, 0.9°, and 1.3°); VCP Gamma also has the same three lowest elevation angles. The closer spacing of lower elevation angles with VCPs Beta and Gamma means that there is a much better chance of an elevation angle scanning a middle- to far-range echo near its top.

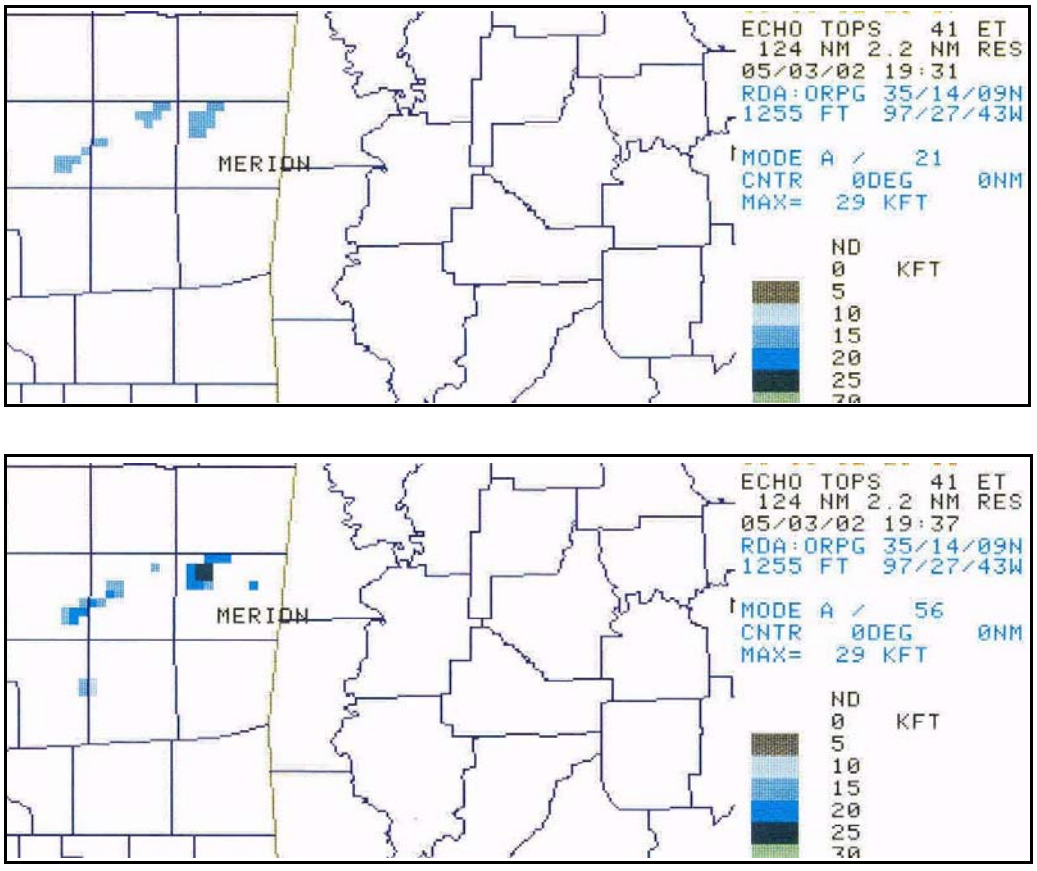

Figure 11. Comparison of echo tops using KBIX for (top) VCP 21 at 1931 UTC and (bottom) VCP Beta at 1937 UTC.

d. Cell tracks

There were three relatively long-lived cells that were in suitable locations to be tracked by KBIX and one of the other radars. Figure 12 shows tracks of the first cell, which was a long-lived hailstorm on 9 May 2002 that moved from west-central to central Mississippi; locations of *Storm Data* reports of hail are indicated. Range from KBIX and KLIX decreased from 320-340 km (170-180 n mi) to 260-270 km (140-145 n mi) as the storm moved east-southeastward. The storm cell was identified about 20 min longer using VCP Beta (KBIX) than using VCP 21 (KLIX). Even though a long-lived hailstorm should consist of a number of cells, the SCIT Algorithm identified only one cell in the KBIX data and two cells in the KLIX data during the storm's three-hour lifetime. With the radar beam being so broad (half-power beamwidth of 4-6 km or 2-3 n mi), there evidently was not sufficient resolution to resolve individual cell evolution.

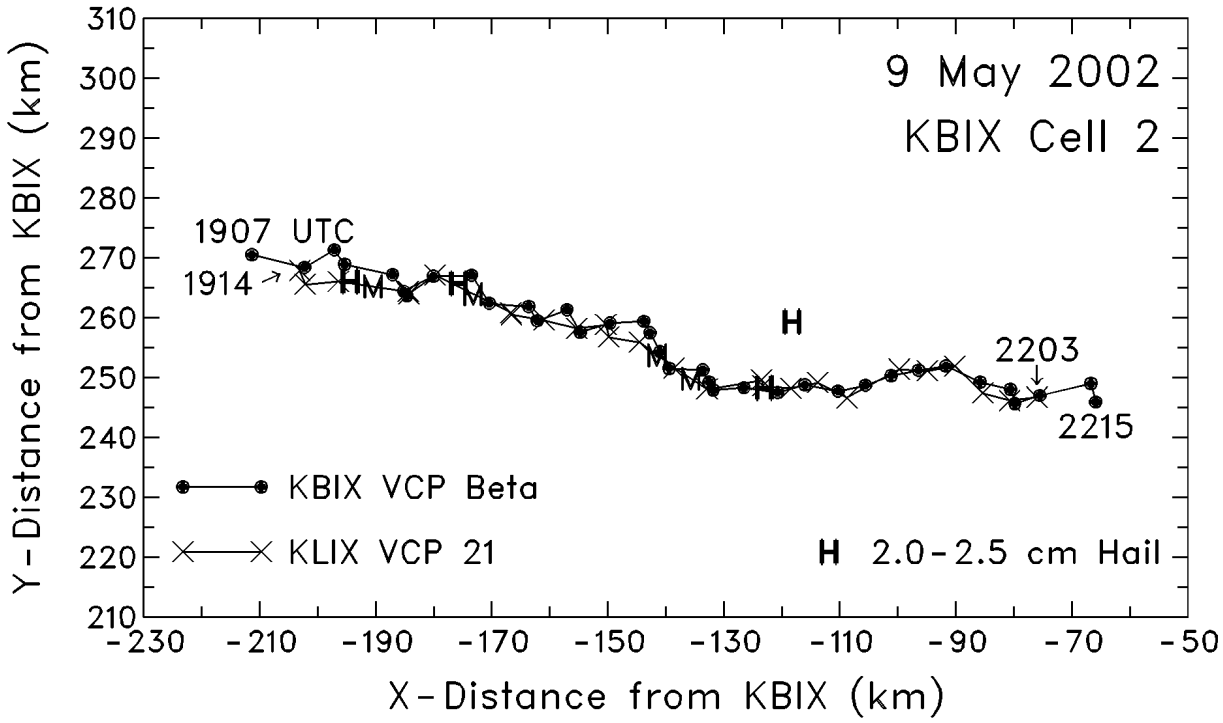

Figure 12. SCIT tracks of a cell based on KBIX and KLIX data. Missing KLIX data are indicated by Ms. There are four plotted hail reports, three partially hidden along the track.

Tracks of a second cell, KBIX Cell 9 on 17 May 2002, are shown in Fig. 13. The cell remained equidistant from KBIX (VCP Beta) and KMOB (VCP 21) as it moved north-northeastward through southeastern Mississippi, approaching the Alabama border. Though no severe weather was reported with the cell, the Hail Detection Algorithm indicated up to

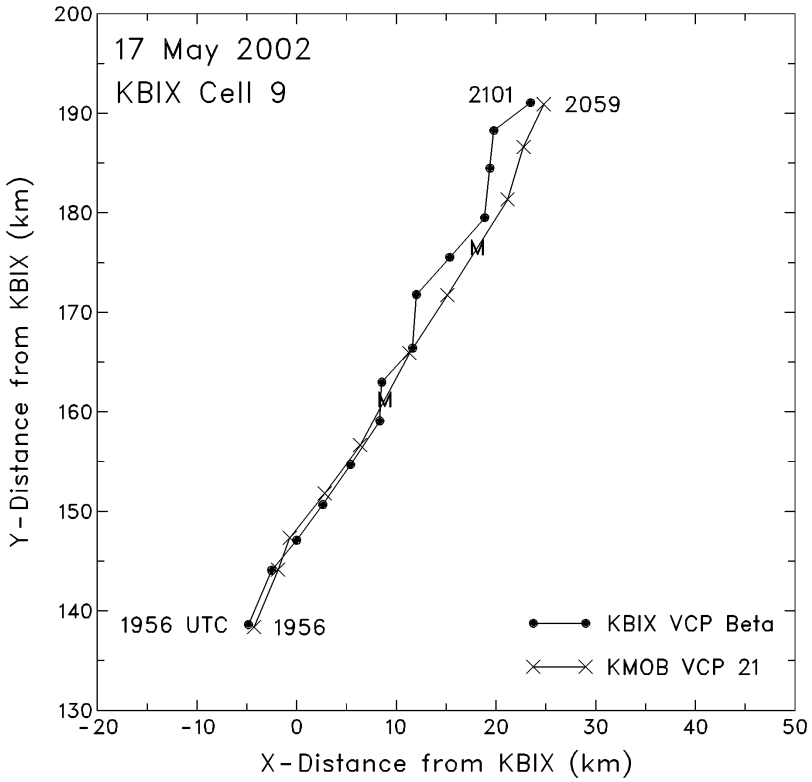

Figure 13. SCIT tracks of a cell based on KBIX and KMOB data. Missing KMOB data are indicated by Ms.

90-100% probability of hail and up to 50-70% probability of severe hail with maximum hail sizes of 1.0-1.25 in (2.5-3.0 cm) expected based on both KBIX and KMOB measurements.

Figure 14 shows tracks of a third severe storm in northeastern Mississippi identified by the SCIT Algorithm using KBIX and KMOB data. At 2028 UTC (beginning of a KBIX data tape), SCIT identified the storm using data collected with VCP Beta. Since maximum reflectivity at that time was 56 dBZ, the storm obviously had been in existence for some time. When observers in the control room changed from VCP Beta to VCP 11 for three volume scans, SCIT no longer identified the storm (Fig. 14 shows interpolated positions in parentheses). When KBIX resumed using VCP Beta, the storm was again identified. However, it was not until 2100--likely 45-60 min after the storm formed--that SCIT identified the storm with the KMOB radar using VCP 21. At 2100 the storm was already severe, with a report of 60 mph winds at 2105. During the next 40 min there were reports of 100 mph winds at Columbus Air Force Base and of 1 in (2.5 cm) hail elsewhere.

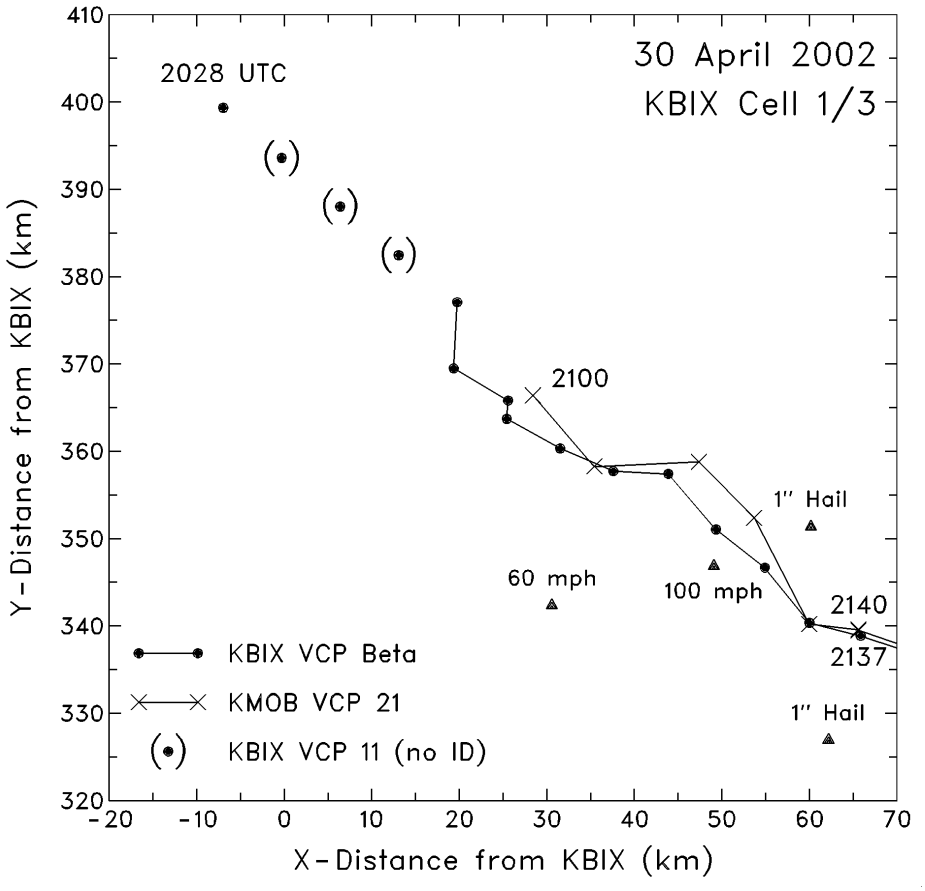

Figure 14. SCIT tracks of a severe storm based on KBIX and KMOB measurements. Triangles indicate the locations of severe weather reports associated with the storm. Dots in parentheses are linearly interpolated positions.

The reason for there initially being no SCIT identification of the storm with VCPs 11 (KBIX) and 21 (KMOB) in Fig. 14 is evident from the displays in Figs. 15 and 16, which are positioned in the vertical relative to height above ground. Figure 15 shows KBIX reflectivity displays for VCP Beta at 2028 UTC and Fig. 16 shows KBIX reflectivity displays for VCP 11 four minutes later. Figure 15 indicates that storm top extended to about 1.3° elevation. With there being data for at least two elevation angles using VCP Beta, the SCIT Algorithm could identify and track the storm. However, with the storm being detected at only one elevation angle with VCP 11, it was not identified by the SCIT Algorithm. For the same reason, the storm was not identified by the algorithm with KMOB using VCP 21 until after the storm moved close enough to the radar for the storm to be detected at two elevation angles.

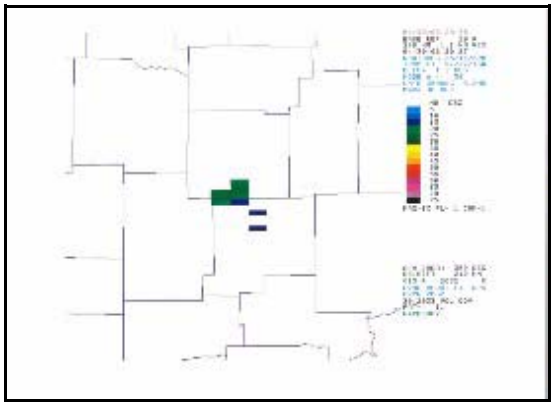

1.3º

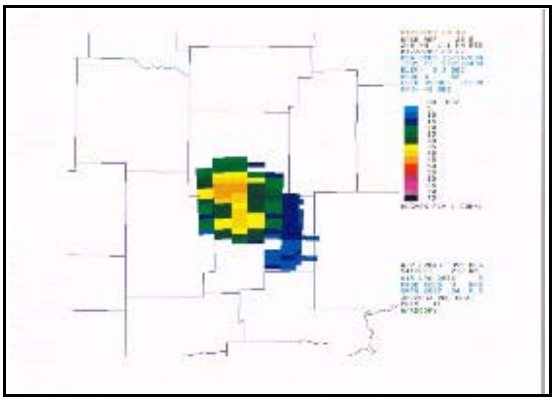

0.9º

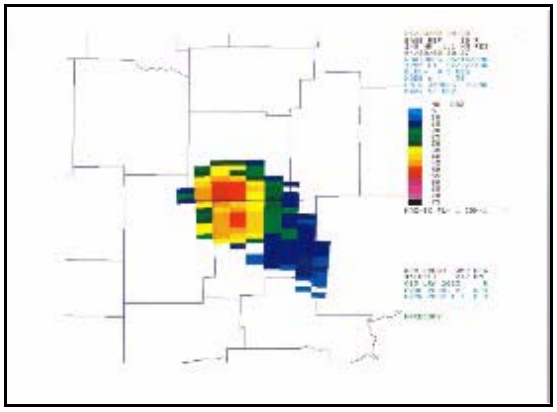

0.5º

Figure 15. KBIX elevation angles of 0.5º (bottom), 0.9º (middle), and 1.3º (top) associated with VCP Beta at 2028 UTC on 30 April 2002.

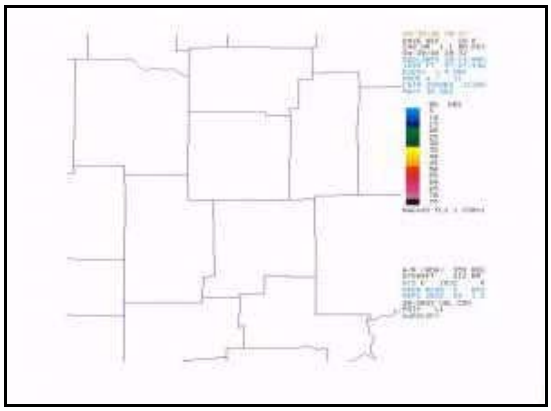

1.5º

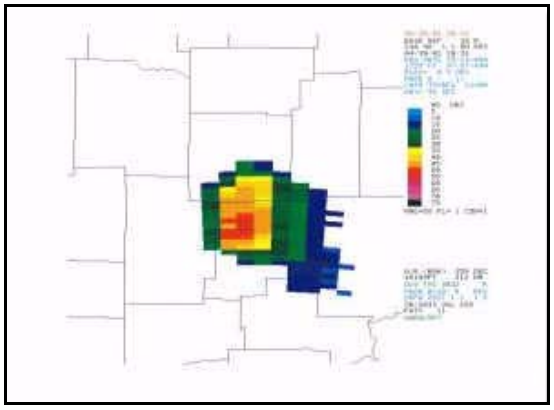

0.5º

Figure 16. KBIX elevation angles of 0.5º (bottom) and 1.5º (top) associated with VCP 11 at 2032 UTC on 30 April 2002.

Data collected on this storm clearly indicate that the finer vertical resolution of VCP Beta makes the difference between algorithm identification and nonidentification. The capability to make finer resolution measurements at lower elevation angles (as exemplified by VCPs Beta and Gamma) becomes especially crucial when one WSR-88D is inoperative and a radar farther away is required to provide the information needed for preparing warnings.

e. Vertically integrated liquid (VIL)

Values of both cell-based VIL and grid-based VIL were available for this study. Cell-based VIL values, computed from the maximum reflectivity at each elevation angle within a cell, were available over the full 460 km (250 n mi) range of reflectivity data. On the other hand, grid-based VIL values, computed from the maximum reflectivity at each elevation angle within a vertical column having horizontal dimensions of 4 km x 4 km, were available only over the first 230 km (125 n mi). VIL values derived using current and experimental VCPs were compared by subtracting the values based on the current VCPs (KLIX, KJAN, KMOB) from the values based on the experimental VCPs (KBIX).

Plots of the cell-based VIL differences and grid-based VIL differences are found in Figs. 17 and 18, respectively. Since VIL is a function of the vertical distribution of reflectivity values, one would expect some relationship between the maximum reflectivity differences in Fig. 9 and the VIL differences in Figs. 17 and 18. The plots indeed indicate that radar-to-radar biases found in Fig. 9 also are evident in Figs. 17 and 18. The means

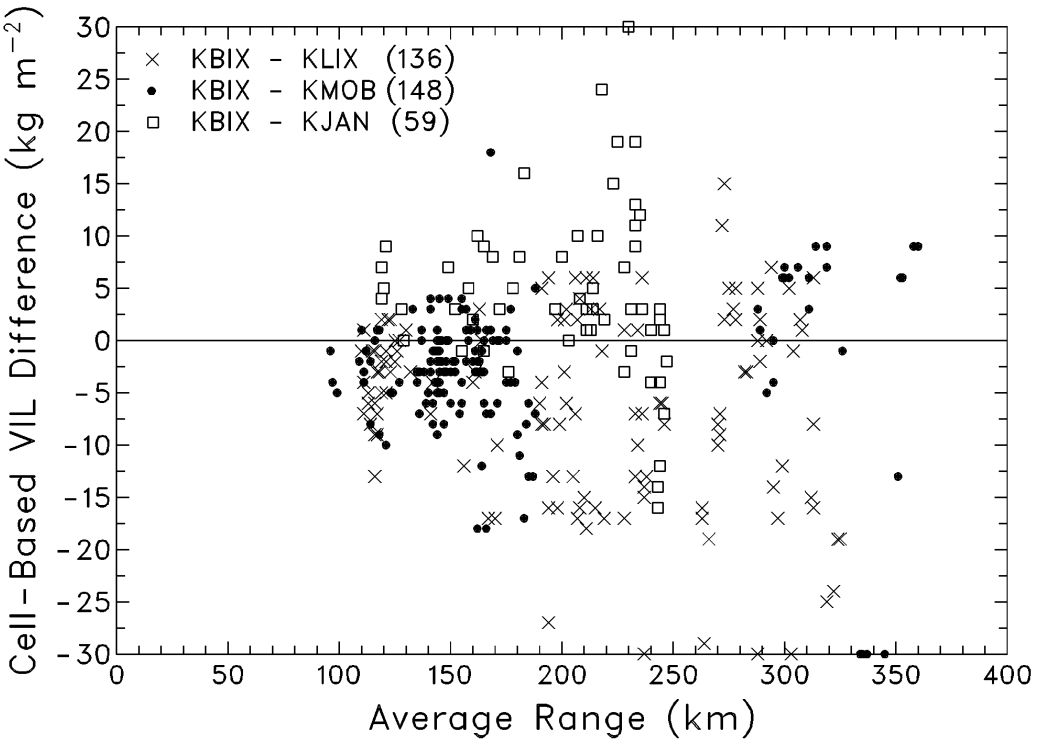

Figure 17. Scatter plot, as a function of average range, of the differences in the maximum cell-based VIL value in a given cell between KBIX and each of the three nearby radars. The number of difference values for each radar pair is indicated in parentheses.

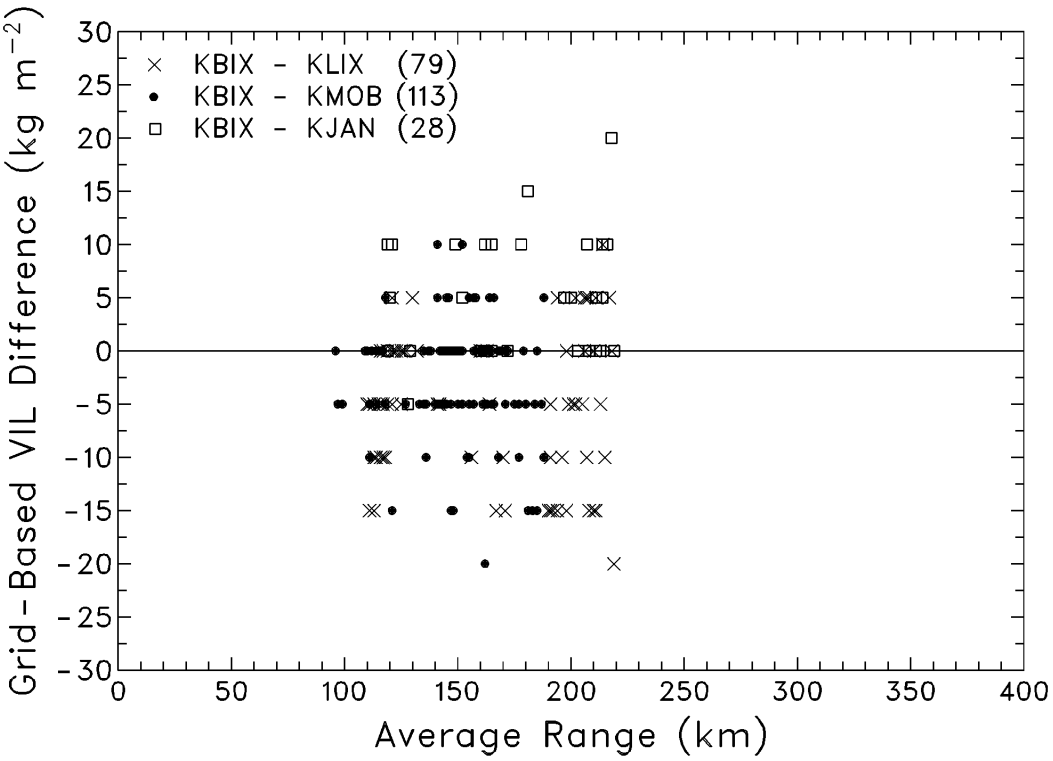

Figure 18. Same as Fig. 17, except for grid-based VIL. VIL values were read from a display where the digitized resolution was 5 kg m^{-2}.

and standard deviations of the various differences are indicated in Tables 3 and 4. In the mean, KBIX values are less than KLIX and KMOB values and greater than KJAN values. The fact that there is not a linear relationship between reflectivity and VIL is reflected in the proportionately different mean difference values between Table 1 and Tables 3 and 4.

Table 3. Means and standard deviations of cell-based VIL differences between KBIX and nearby WSR-88Ds.

Radar Pair	Mean Difference	Standard Deviation
KBIX-KLIX	-5.85 kg m^{-2}	8.93 kg m^{-2}
KBIX-KMOB	-2.70 kg m^{-2}	6.99 kg m^{-2}
KBIX-KJAN	4.34 kg m^{-2}	8.13 kg m^{-2}

Table 4. Means and standard deviations of grid-based VIL differences between KBIX and nearby WSR-88Ds.

Radar Pair	Mean Difference	Standard Deviation
KBIX-KLIX	-5.13 kg m^{-2}	6.65 kg m^{-2}
KBIX-KMOB	-2.90 kg m^{-2}	5.21 kg m^{-2}
KBIX-KJAN	5.36 kg m^{-2}	5.76 kg m^{-2}

f. Hail

Comparisons were made for three parameters from the Hail Detection Algorithm (HDA): maximum hail size, probability of hail (POH), and probability of severe hail (POSH). In order not to bias the comparisons with an unrealistic number of zero differences, no comparisons were made for cells when both KBIX and the equidistant radar gave zero probability for occurrence of hail.

Comparisons for maximum hail size are shown in Fig. 19. There are too few data points to determine whether there are different biases for the various radar comparisons. Consequently, the mean and standard deviation of size difference were computed for all three data sets combined. The results are given in Table 5. As suggested by the distribution of data points in Fig. 19, the mean difference is essentially zero.

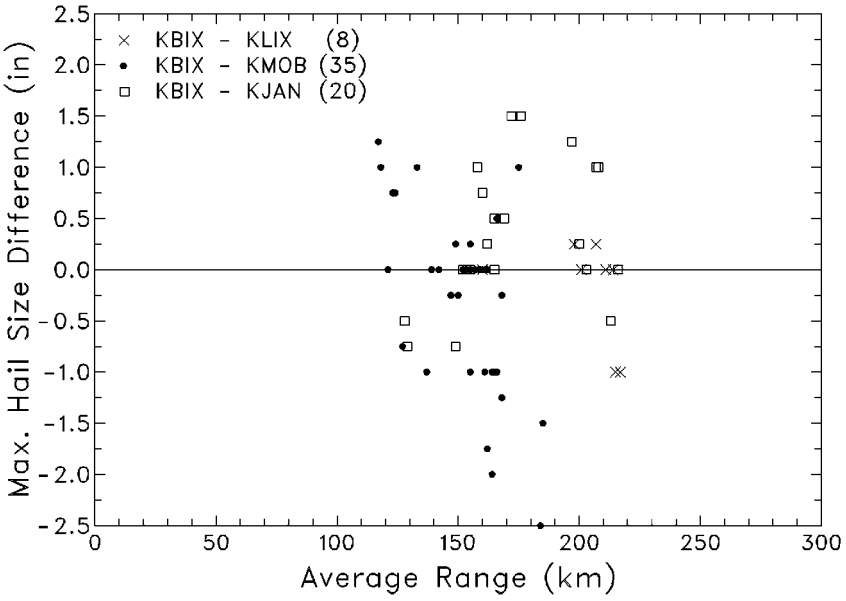

Figure 19. Scatter plot, as a function of average range, of the differences in maximum hail size in a given cell between KBIX and each of the three nearby radars. The number of difference values for each radar pair is indicated in parentheses.

Comparisons of POH and POSH are given in Figs. 20 and 21, respectively. As with maximum hail size, there are too few POH and POSH data points to say anything significant about differences between individual pairs of radars. The means and standard deviations

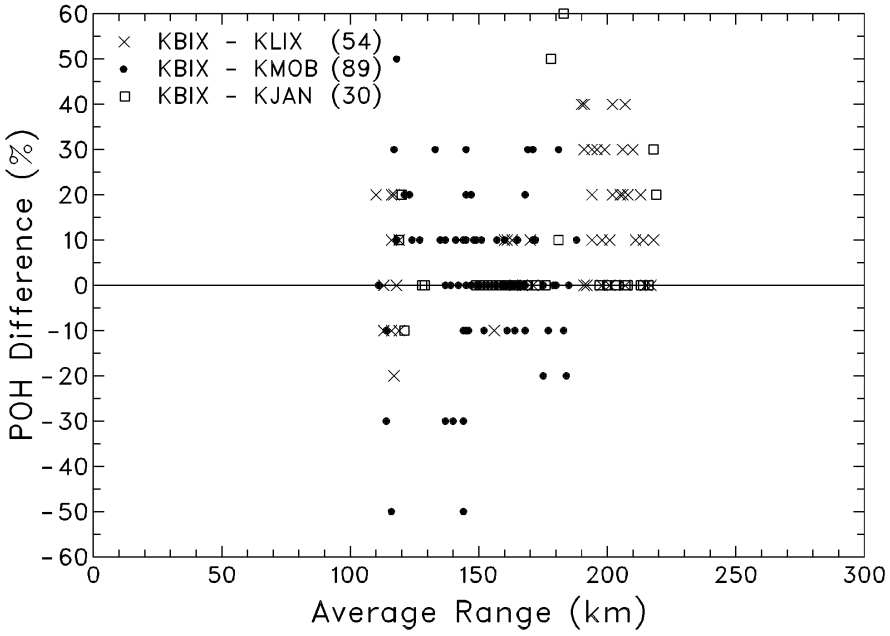

Figure 20. Same as Fig. 19, except for probability of hail (POH).

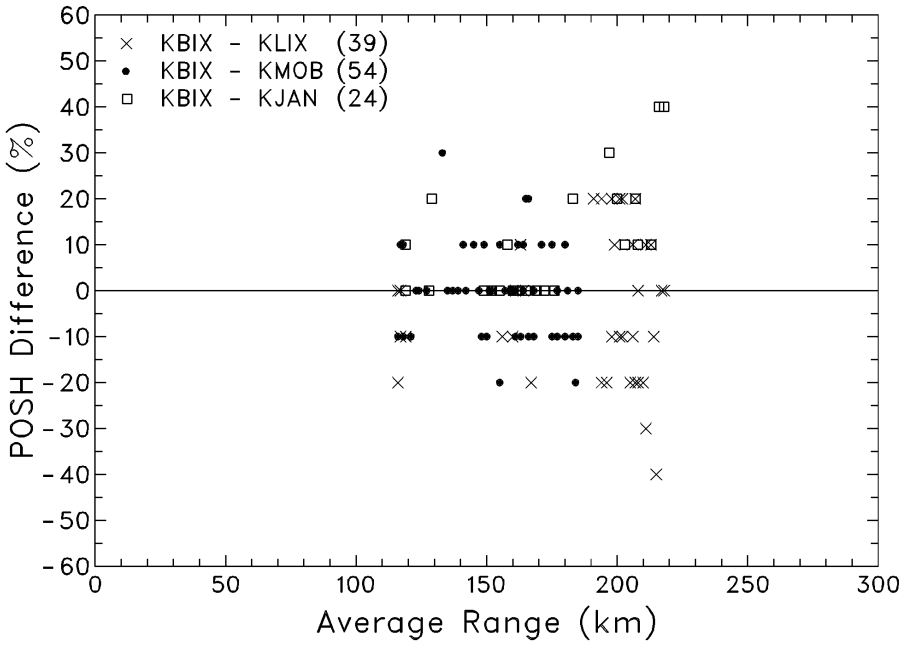

Figure 21. Same as Fig. 19, except for probability of severe hail (POSH).

for POH and POSH differences are given in Table 5. The mean differences of probability values between KBIX and the nearby radars are about 6% and 1% for POH and POSH, respectively. The standard deviations are nearly identical (14-16%).

Table 5. Means and standard deviations of HDA parameter differences between KBIX and all of the nearby WSR-88Ds.

Parameter	Data Points	Mean Diff.	Stand. Dev.
Max. Size	63	-0.07 in (-0.17 cm)	0.84 in (2.13 cm)
POH	173	5.66 %	16.04 %
POSH	117	0.94 %	13.58 %

Attempts were made to relate *Storm Data* hail reports with output from HDA. Except for the storm situation shown in Fig. 5, cells associated with *Storm Data* reports either were outside the coverage areas indicated in Fig. 4 or they were located beyond the maximum algorithm distance of 230 km (as for the cases shown in Figs. 12 and 14). Figure 22 shows the evolution of three HDA parameters associated with the same cell that produced the circulations in Fig. 5. Even though the SCIT Algorithm identified the same cell in the KBIX data for over three hours, it is evident from the curves in Fig. 22 that a series of closely-spaced cells was tracked.

The closeness of agreement between the POH curves is remarkable. POH values differ by no more than 10% for the KBIX-KMOB portion of the curves (up through 2000) and are in complete agreement along the KBIX-KJAN portion of the curves, where POH values remained a constant 100%. Except for a brief time period from about 1940 through 2000, the POSH curves rarely differed by more than 10%. The most obvious differences between pairs of curves in Fig. 22 are for maximum hail size. It is common to find differences of 1 in or more, which suggests that maximum hail size is a difficult parameter to predict.

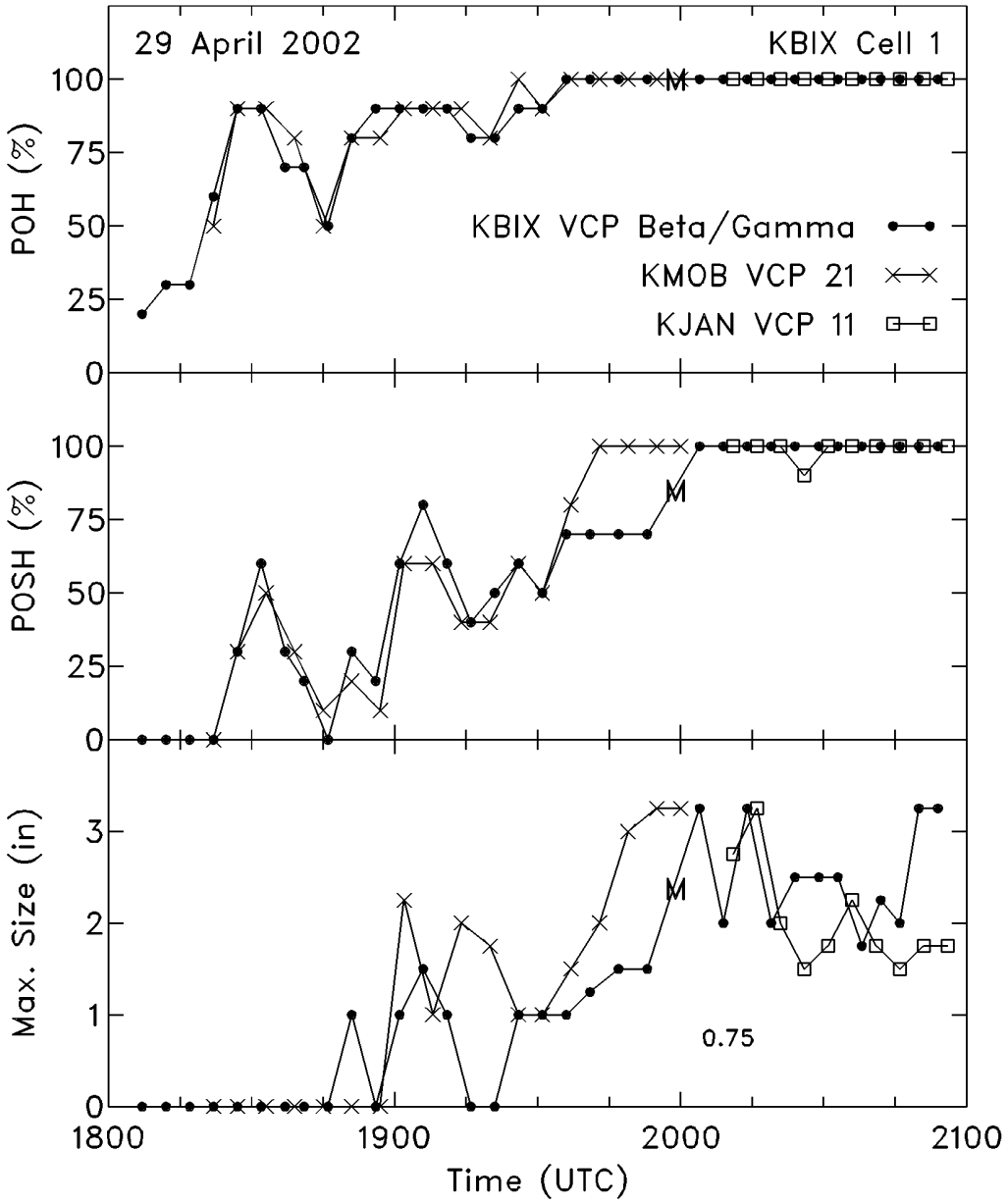

Figure 22. Temporal variation of POH, POSH, and maximum hail size in KBIX Cell 1 on 29 April 2002 (associated with KBIX Meso 625 in Fig. 5). Comparisons between KBIX and KMOB are made through 2000 and between KBIX and KJAN thereafter. Ranges from the radars varied from 140-190 km. The only Storm Data *hail report with the storm was for 0.75 in (2 cm) hail at 2010 UTC about 10 km south of the cell track.*

5. Discussion

A basic characteristic of the experimental VCPs is closer spacing of lower elevation angles. This characteristic leads to a number of advantages for the forecaster. For example, blocking of lower elevation angles by terrain produces underestimates of surface precipitation rates because the lowest useable elevation angle is a considerable distance above ground. Current VCPs place the first useable elevation angle 0.9-1.0° above the highest blocked angle, whereas experimental VCPs place the first useable elevation angle only 0.4-0.5° above the highest blocked angle. Thus, measurements closer to the ground would result in more realistic estimates of surface precipitation rates. The precipitation advantages could not be confirmed during this field test because the current precipitation algorithm accepts only elevation angles specified by current VCPs 11 and 21.

Comparisons in this study were undertaken for storms that were essentially equidistant between KBIX and one of the nearby WSR-88Ds. Owing to the relative locations of the radars, comparisons were made only for those storms beyond about 100 km (55 n mi). The comparisons presented in this report clearly show advantages of experimental VCPs over current VCPs. With greater vertical data density at lower elevation angles associated with the experimental VCPs, a developing storm and its associated rotation characteristics are identified by the algorithms up to 10-35 min earlier because vertical continuity requirements are satisfied sooner. This means that information about mesocyclone and tornadic vortex signatures and parameters such as storm location and tracking, maximum reflectivity, vertically integrated liquid (VIL), probability of hail and severe hail, expected maximum hail size, etc. become available to forecasters much earlier in a storm's lifetime.

Of the three experimental VCPs evaluated in this report, the one that would have most day-to-day impact on the operational community is VCP Gamma. VCP Gamma is a faster version of VCP 11 with the same number of elevation scans, but with elevation angles moved downward to provide better estimates of surface precipitation rates, better confirmation of microburst and tornadic vortex signatures, and better identification of more distant severe storms. Virtually all examples presented in this report are, by chance, for VCP Beta. However, the VCP Beta results for these mid- to far-range storms represent what would have been measured by VCP Gamma, because the lowest five elevation angles are comparable for the two VCPs. Therefore, it is logical that VCP Gamma, which scans to higher elevation angles than VCP Beta, should be the first of the experimental VCPs to be implemented for operational WSR-88Ds to monitor storms at all ranges.

Acknowledgments. Success of the field test was based on the dedication of staff members from the ROC, NSSL, NWS Warning Decision Training Branch, NWS Forecast Office in Jackson, MS, and Keesler Air Force Base. Randy Steadham (ROC), who capably directed the field test, kindly provided the radar display images.